

Energy loss of heavy quarks and B and D meson spectra in PbPb collisions at LHC energies

Kapil Saraswat^a, Prashant Shukla^{b,c,*}, Vineet Kumar^b, Venktesh Singh^a

^a*Department of Physics, Banaras Hindu University, Varanasi 221005, India.*

^b*Nuclear Physics Division, Bhabha Atomic Research Centre, Mumbai 400085, India.*

^c*Homi Bhabha National Institute, Anushakti Nagar, Mumbai 400094, India.*

Abstract

We study the production and evolution of charm and bottom quarks in hot partonic medium produced in heavy ion collisions. The heavy quarks loose energy in the medium which is reflected in the transverse momentum spectra of heavy mesons. The collisional energy loss of heavy quarks has been calculated using QCD calculations. The radiative energy loss is obtained using two models namely reaction operator formalism and generalized dead cone approach. The nuclear modification factors, R_{AA} as a function of transverse momentum by including shadowing and energy loss are calculated for D^0 and B^+ mesons in PbPb collisions at $\sqrt{s_{NN}} = 5.02$ TeV and for D^0 mesons at $\sqrt{s_{NN}} = 2.76$ TeV and are compared with the recent measurements. The radiative energy loss from generalized dead cone approach alone is sufficient to produce measured D^0 meson R_{AA} at both the LHC energies. The radiative energy loss from reaction operator formalism plus collisional energy loss gives good description of D^0 meson R_{AA} . For the case of B^+ meson, the radiative energy loss from generalized dead cone approach plus collisional energy loss gives good description of the CMS data. The radiative process is dominant for charm quarks while for the bottom, both the radiative process and the elastic collisions are important.

Keywords: QGP, heavy quark energy loss, radiative and collisional energy loss

*Corresponding author

Email address: pshuklabarc@gmail.com (Prashant Shukla)

1. Introduction

The heavy ion collisions at Relativistic Heavy Ion Collider (RHIC) and Large Hadron Collider (LHC) are performed to create and characterize Quark Gluon Plasma (QGP). The properties of QGP are studied through variety of probes accessible in these experiments [1]. The heavy (charm and bottom) quarks are the best probes of the transport properties of the medium. Since the heavy quarks are produced in hard partonic interactions in heavy ion collisions, their initial momentum distribution can be calculated from pQCD [2, 3, 4]. While traversing the hot/dense medium formed in the collisions, these quarks loose energy due to the elastic collisions with the plasma constituents and/or by radiating a gluon. There are several formulations to calculate collisional [5, 6, 7, 8, 9] as well as radiative energy loss [10, 11, 12, 13]. For a review of many of these formalism see Ref. [14, 15]. The collisional energy loss dominates at low parton energy but the radiative energy loss dominates over the collisional energy loss at high parton energy [16]. A recent work in Ref. [17] finds significant non-perturbative contribution to collision energy loss accompanying a pion production in quark - gluon - pion interaction.

The ALICE experiment measured nuclear modification factor (R_{AA}) [18] and elliptic flow [19, 20] of D mesons in PbPb collisions at $\sqrt{s_{NN}} = 2.76$ TeV. Many transport models employing heavy quark dynamics have been used to interpret this data [21, 22, 23, 24] which we summarize in the following. A Boltzmann Approach to MultiParton Scatterings (BAMPS) [21] is a transport model which describes the D meson data very well. The model lacks the radiative energy loss which is accounted for by multiplying the collision cross-section by 3.5. The POWLANG is a Monte Carlo model [22] where the initial heavy quarks pairs are produced by POWHEG-BOX and their propagation in hydrodynamically expanding medium is simulated through Langevin equation. The hydrodynamic model from Ref. [23] uses a modified Langevin equation with terms for collisional and radiative interactions. The transport coefficients are then tuned to produce the D meson R_{AA} at $\sqrt{s_{NN}} = 2.76$ TeV. In Parton-Hadron-String Dynamics

(PHSD) transport approach [24], the initial charm quarks are produced by tuned PYTHIA which scatter with the off shell partons whose masses and widths are given by the Dynamical Quasi Particle Model (DQPM). In this model, radiative process is suppressed due to large gluon mass in DQPM. HYDJET++ model [25, 26] is a Monte Carlo model which includes collision energy loss calculated in the high momentum limit and the radiative energy loss is obtained by generalization of BDMPS (Baier, Dokshitzer, Mueller, Peigne and Schiff) model based on dead cone approximation.

The R_{AA} of B meson via its decay to J/ψ was measured by the CMS experiment [27]. The measurements of both D and B at LHC and D at RHIC are used to constrain energy loss formalisms in our simple hydrodynamic model by modifying the transverse momentum (p_T) spectra of heavy quarks due to collision and radiative energy loss [28]. ALICE and CMS recently updated D meson R_{AA} in extended p_T [29] and centrality [30] range in PbPb collisions at $\sqrt{s_{NN}} = 2.76$ TeV. CMS has published good quality measurements of R_{AA} of D^0 [31] and B^+ [32] mesons and elliptic flow, v_2 of D^0 mesons [33] in PbPb collision at $\sqrt{s_{NN}} = 5.02$ TeV. These new LHC data can be used to test various models of heavy quark energy loss.

In this work, first we calculate the p_T spectra of heavy mesons in pp collision at $\sqrt{s} = 5.02$ TeV using pQCD model [2, 3] and make a comparison with D^0 and B^+ meson measurements of CMS. The radiative energy loss of charm and bottom quarks are calculated using reaction operator formalism DGLV (Djordjevic, Gyulassy, Levai and Vitev) [12, 13, 34] and generalized dead cone approach [28, 35]. The collisional energy loss is calculated using Peigne and Peshier formalism [9]. The nuclear modification factors including shadowing and energy loss are calculated for D^0 and B^+ mesons in PbPb collision at $\sqrt{s_{NN}} = 5.02$ TeV and are compared with the CMS measurements. We also calculate R_{AA} for D^0 meson in PbPb collision at $\sqrt{s_{NN}} = 2.76$ TeV to compare with the updated data from ALICE and CMS.

2. Heavy Quark Production

The heavy quarks are produced by the processes $q + \bar{q} \rightarrow Q + \bar{Q}$ and $g + g \rightarrow Q + \bar{Q}$ in the pp collisions as

$$p(P_1) + p(P_2) \rightarrow Q(p_1) + \bar{Q}(p_2) + X . \quad (1)$$

The hadronic kinematic variables are

$$\begin{aligned} S &= (P_1 + P_2)^2, \\ T_1 &= (P_1 - p_1)^2 - m^2 = -\sqrt{S} m_T e^y, \\ U_1 &= (P_1 - p_2)^2 - m^2 = -\sqrt{S} m_T e^{-y}, \end{aligned} \quad (2)$$

where y is the rapidity, $m_T (= \sqrt{p_T^2 + m^2})$ is the transverse mass, p_T is the transverse momentum and m is the mass of heavy quark. The cross section for the process given in Eq. 1 is

$$S^2 \frac{d^2\sigma(S, T_1, U_1)}{dT_1 dU_1} = k \sum_{i,j} \int \frac{dx_1}{x_1} \int \frac{dx_2}{x_2} f_i^p(x_1, Q^2) f_j^p(x_2, Q^2) s^2 \frac{d^2\sigma_{ij}(s, t_1, u_1)}{dt_1 du_1} . \quad (3)$$

Here, $s = x_1 x_2 S$, $t_1 = x_1 T_1$, $u_1 = x_2 U_1$ are partonic variables. The functions $f_i^p(x_1, Q^2)$ denote the parton distribution functions (PDFs) in nucleons. We take $Q = m_T$ and the k factor is adjusted to reproduce the data. The mass of charm (bottom) quark is taken as 1.50 (5.0) GeV. The Born cross section in 4 dimensions for gg and $q\bar{q}$ interaction can be written in the following form

$$s^2 \frac{d^2\sigma_{ij}}{dt_1 du_1} = \delta(s + t_1 + u_1) \times \sigma_{ij}(s, t_1, u_1) . \quad (4)$$

From Eqs. 3 and 4

$$\frac{d^2\sigma_{pp}}{dp_T^2 dy} = \frac{k}{S} \sum_{i,j} \int_{x_{1-}}^1 \frac{dx_1}{x_1} \left(-\frac{1}{t_1} \right) f_i^p(x_1, Q^2) f_j^p(x_2, Q^2) \sigma_{ij}(s, t_1, u_1) . \quad (5)$$

Here, $x_{1-} = -U_1/(S + T_1)$ and $x_2 = -x_1 T_1/(x_1 S + U_1)$. The Born cross sections σ_{ij} calculated upto LO are given in the appendix.

CT10 parton density functions [36] are used in the present calculations. The spatially dependent EPS09s sets [37] are used to calculate the modifications

of the PDFs inside nucleus. The differential cross section including nuclear shadowing effect corresponding to a centrality class between impact parameters b_1 and b_2 is calculated as

$$\frac{d^2\sigma_{\text{sh}}(b_1, b_2)}{dp_T^2 dy} = \frac{k}{S} \sum_{i,j} \int_{x_{1-}}^1 \frac{dx_1}{x_1} \left(-\frac{1}{t_1} \right) \sigma_{ij}(s, t_1, u_1) \frac{1}{AB} \sum_{n,m=0}^4 T_{AB}^{nm}(b_1, b_2) c_n^i(x_1, Q^2) f_i^A(x_1, Q^2) c_m^j(x_2, Q^2) f_j^B(x_2, Q^2), \quad (6)$$

where the bound state PDFs $f_{i,j}^{A,B}$, the function T_{AB}^{nm} and the coefficients $c_{n,m}^{i,j}$ are given in EPS09s sets [37]. The spectrum in PbPb collisions is then obtained by including the momentum loss Δp_T in the p_T spectrum given in Eq. 6.

Single heavy meson production cross sections for both the pp and PbPb collisions are obtained by convoluting the heavy quark production cross section with the fragmentation function $D_Q^h(z)$ [38] as

$$\frac{d^2\sigma^h}{d(p_T^h)^2 dy} = f_{\text{meson}} \int_0^1 dz \frac{D_Q^h(z)}{z^2} \frac{d^2\sigma}{dp_T^2 dy}. \quad (7)$$

Here, $z = p_T^h/p_T$ and f_{meson} is the fragmentation fraction for the heavy meson. We take f_{meson} as 0.557 for D^0 meson [39, 40] and 0.402 for B^+ meson [32]. Peterson fragmentation function is used for $D_Q^h(z)$ [41] which is given as follows

$$D_Q^h(z) = \frac{N}{z \left[1 - \frac{1}{z} - \frac{\epsilon_Q}{(1-z)} \right]^2}. \quad (8)$$

We take $\epsilon_c = 0.016$ and $\epsilon_b = 0.0012$ and N is the normalization constant.

Finally, the nuclear modification factor R_{AA} is calculated as

$$R_{AA}(p_T^h, b_1, b_2) = \frac{d^2\sigma_{PbPb}^h(p_T^h, b_1, b_2)}{d(p_T^h)^2 dy} \bigg/ \int_{b_1}^{b_2} d^2b T_{AA} \frac{d^2\sigma_{pp}^h(p_T^h)}{d(p_T^h)^2 dy}. \quad (9)$$

Here, T_{AA} is the nuclear overlapping function.

3. Heavy Quark Energy Loss

For the collisional energy loss we use the formalism of Peigne and Peshier (PP) [9]. The radiative energy loss is calculated using the reaction operator

formalism (DGLV) [12, 13, 34] and using the generalized dead cone approach [35]. The DGLV formalism is based on a systematic expansion of the energy loss in terms of the number of the scatterings experienced by the propagating parton. In the single hard scattering limit, only the leading term in the expansion is included. The Generalised dead cone approach is an extension of the Gunion Bertsch formalism [42]. The Gunion Bertsch formula for light quarks energy loss was extended to heavy quarks by introducing the mass in the matrix element but only within the small angle approximation [43]. Due to this mass effect, the soft gluon emission from a heavy quark was suppressed in comparison to that from a light quark which is known as the dead cone effect. In the generalized dead-cone approach the probability of gluon emission off a heavy quark is obtained by relaxing some of the constraints such as the gluon emission angle and the scaled mass of the heavy quark with its energy. Using the same assumptions as generalized dead cone approach [35] we calculated the energy loss expression [28] given as

$$\frac{dE}{dx} = 24 \alpha_s^3 \rho_{QGP} \frac{1}{\mu_g} (1 - \beta_1) \left(\sqrt{\frac{1}{(1 - \beta_1)} \log\left(\frac{1}{\beta_1}\right)} - 1 \right) \mathcal{F}(\delta) . \quad (10)$$

Here,

$$\begin{aligned} \mathcal{F}(\delta) &= 2\delta - \frac{1}{2} \log\left(\frac{1 + \frac{M^2}{s} e^{2\delta}}{1 + \frac{M^2}{s} e^{-2\delta}}\right) - \left(\frac{\frac{M^2}{s} \sinh(2\delta)}{1 + 2 \frac{M^2}{s} \cosh(2\delta) + \frac{M^4}{s^2}}\right) , \\ \delta &= \frac{1}{2} \log\left[\frac{1}{(1 - \beta_1)} \log\left(\frac{1}{\beta_1}\right) \left(1 + \sqrt{1 - \frac{(1 - \beta_1)}{\log\left(\frac{1}{\beta_1}\right)}}\right)^2\right] , \\ s &= 2E^2 + 2E\sqrt{E^2 - M^2} - M^2 , \quad \beta_1 = \mu_g^2/(C E T) , \\ C &= \frac{3}{2} - \frac{M^2}{4 E T} + \frac{M^4}{48 E^2 T^2 \beta_0} \log\left[\frac{M^2 + 6 E T (1 + \beta_0)}{M^2 + 6 E T (1 - \beta_0)}\right] , \\ \beta_0 &= \sqrt{1 - \frac{M^2}{E^2}} , \quad \rho_{QGP} = \rho_q + \frac{9}{4} \rho_g , \\ \rho_q &= 16T^3 \frac{1.202}{\pi^2} , \quad \rho_g = 9N_f T^3 \frac{1.202}{\pi^2} . \end{aligned} \quad (11)$$

$\mu_g = \sqrt{4\pi\alpha_s T^2 (1 + N_f/6)}$ is the Debye screening mass, T is the temperature of the QGP medium, $\alpha_s (= 0.3)$ is the fine structure splitting constant for strong interaction and $N_f (= 3)$ is the number of quark flavours.

4. Model For QGP Evolution

The average distance L travelled by the heavy quark in the plasma is obtained as per the method described in Ref. [28]. If the velocity of the heavy quark is $v_T = p_T/m_T$, the effective path length L_{eff} is obtained as

$$L_{eff} = \min\left[L, v_T \times \tau_f\right]. \quad (12)$$

The temperature as a function of proper time is obtained for each centrality bin in an isentropic cylindrical expansion scenario with the Lattice QCD and hadronic resonance equations of states [44]. We calculate the energy loss as a function of proper time which is then averaged over the temperature evolution. The measured values of $dN/d\eta$ at $\sqrt{s_{NN}} = 5.02$ TeV [45] and at $\sqrt{s_{NN}} = 2.76$ TeV [46] are used as inputs for a given centrality to calculate the initial temperature. The initial and freeze-out times are taken as 0.3 and 6 fm/c respectively. Various parameters used in our model for different centralities such as average value of impact parameter $\langle b \rangle$, maximum value b_{max} , number of participants N_{part} and the measured $dN/d\eta$ are given in the Table 1 along with the calculated values of L and initial temperature (T_0).

Table 1: Parameters of QGP evolution model

$\sqrt{s_{NN}}$ (TeV)	Centrality class (%)	$\langle b \rangle$ (fm)	b_{max} (fm)	N_{part}	$\frac{dN}{d\eta}$	L (fm)	T_0 (GeV)
5.02	0-10	3.34	5.0	359	1749	5.74	0.508
5.02	0-100	9.65	22.0	114	436	4.18	0.469
2.76	0-10	3.44	5.0	356	1449	5.73	0.467
2.76	0-100	9.68	22.0	113	363	4.16	0.436

5. Results and Discussions

Figure 1 shows the pQCD LO calculation of differential cross section of D^0 mesons as a function of transverse momentum p_T , in pp collision at $\sqrt{s} = 5.02$

TeV compared with the CMS measurements [31]. The calculation with factor $k = 4$ gives good description of the data.

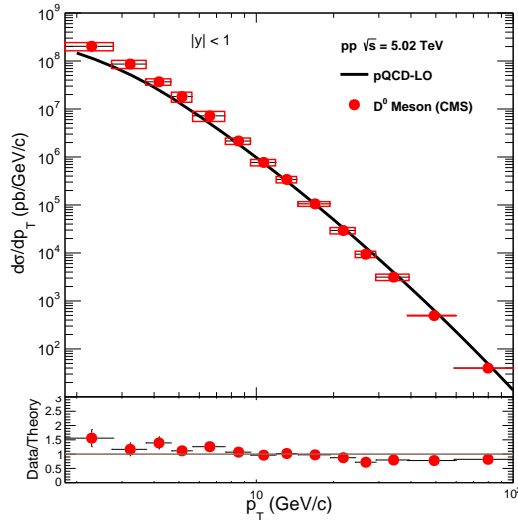


Figure 1: (color online): The pQCD LO calculation of differential cross section of D^0 mesons as a function of the transverse momentum p_T , in pp collision at $\sqrt{s} = 5.02$ TeV. The calculations are compared with the CMS data of D^0 mesons [31].

Figure 2 shows the pQCD LO calculation of differential cross section of B^+ mesons as a function of the transverse momentum p_T , in pp collision at $\sqrt{s} = 5.02$ TeV compared with the CMS measurements [32]. The calculation with factor $k = 5$ gives good description of the data.

Figure 3 shows the energy loss of charm quark as a function of quark energy for the case of 0 - 10 % central PbPb collision at $\sqrt{s_{NN}} = 5.02$ TeV calculated using PP, DGLV and Present formalisms. The radiative energy loss calculated by present approach is larger than that by DGLV. The collisional energy loss calculated by PP formalism is less than the radiative energy loss calculation. Figure 4 is the same as Fig. 3 but for the case of minimum bias PbPb collisions.

Figure 5 shows the energy loss of bottom quark as a function of quark energy for the minimum bias PbPb collisions at $\sqrt{s_{NN}} = 5.02$ TeV using PP, DGLV and Present formalisms. The radiative energy loss calculated by present approach

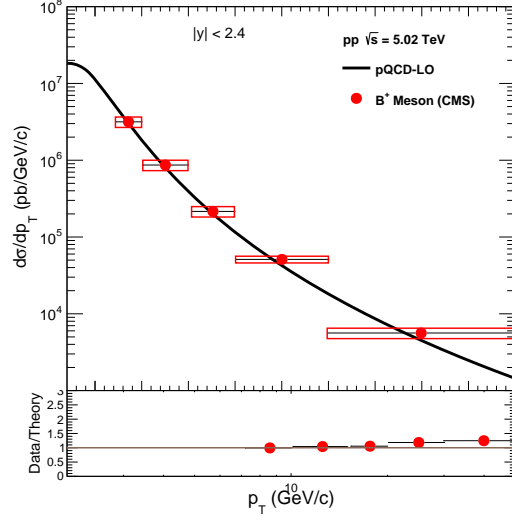


Figure 2: (color online): The pQCD LO calculation of differential cross section of B^+ mesons as a function of the transverse momentum p_T , in pp collision at $\sqrt{s} = 5.02$ TeV. The calculations are compared with the CMS data of B^+ mesons [32].

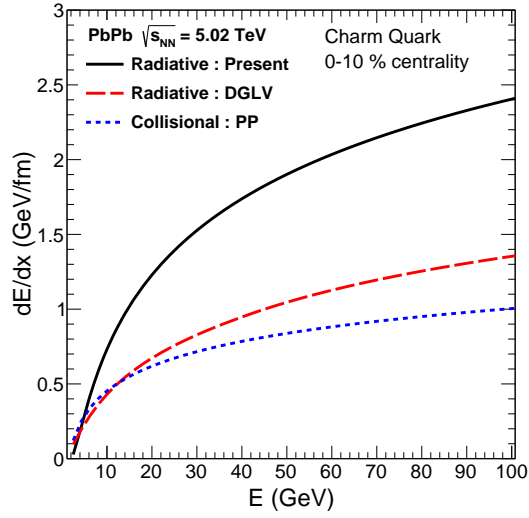


Figure 3: (color online): The energy loss dE/dx as a function of energy E of charm quark obtained using PP, DGLV and Present calculation in 0 - 10 % centrality region for PbPb collision at $\sqrt{s_{NN}} = 5.02$ TeV.

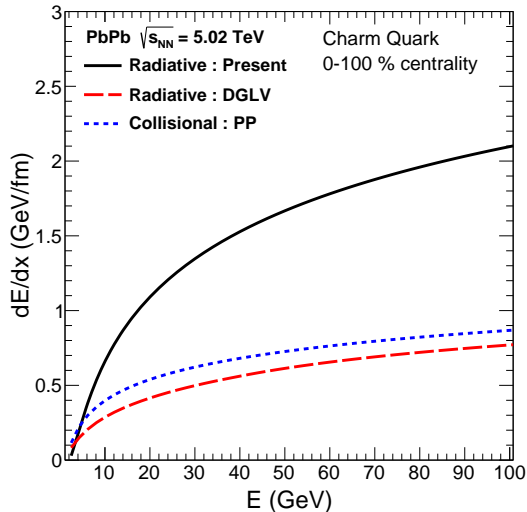


Figure 4: (color online): The energy loss dE/dx as a function of energy E of charm quark obtained using PP, DGLV and Present calculation in 0 - 100 % centrality region for PbPb collision at $\sqrt{s_{NN}} = 5.02$ TeV.

is larger than that by DGLV. The collisional energy loss for the bottom quarks is significant as compared to the radiative energy loss.

The radiative energy loss calculated by the generalized dead cone approach is larger than the energy loss calculated by DGLV. This arises due to different kinematic cuts used in the two formalisms. Namely, in the DGLV formalism the gluon emission is constrained only to the forward angles $\theta < \pi/2$, where as in the generalized dead cone approach, full range of θ is taken care of.

Figure 6 shows the nuclear modification factor R_{AA} of D^0 as a function of the transverse momentum p_T , obtained by including shadowing and energy loss (DGLV, Present, PP + DGLV and PP + Present calculations) for 0 - 10 % central PbPb collision at $\sqrt{s_{NN}} = 5.02$ TeV. The calculations are compared with the CMS data [31]. We observe that the radiative energy loss by present formalism reproduces the data without adding collisional energy loss. The radiative energy loss by DGLV added to the collisional energy loss by PP describes the CMS data at high p_T range. The radiative energy loss by present formalism ad-

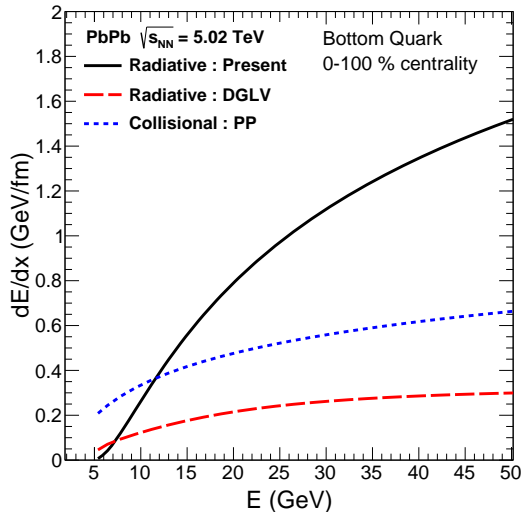


Figure 5: (color online): The energy loss dE/dx as a function of energy E of bottom quark obtained using PP, DGLV and Present calculation in 0 - 100 % centrality region for PbPb collision at $\sqrt{s_{NN}} = 5.02$ TeV.

added to the collisional energy loss by PP formalism overestimates the measured suppression of D^0 meson.

Figure 7 shows the nuclear modification factor R_{AA} of D^0 as a function of the transverse momentum p_T , obtained by including shadowing and energy loss (DGLV, Present, PP + DGLV, PP + Present calculations) for the minimum bias PbPb collision at $\sqrt{s_{NN}} = 5.02$ TeV. The calculations are compared with the CMS data [31]. The radiative energy loss by present formalism describes the CMS data within the uncertainties of the data. The sum of radiative and collisional energy loss (PP + DGLV) gives good description of the data at high p_T . The radiative energy loss by present formalism added to the collisional energy loss by PP formalism overestimates the measured suppression of D^0 meson.

Figure 8 shows the nuclear modification factor R_{AA} of B^+ as a function of the transverse momentum p_T , obtained by including shadowing and energy loss (DGLV, Present, PP + DGLV and PP + Present calculations) for the minimum

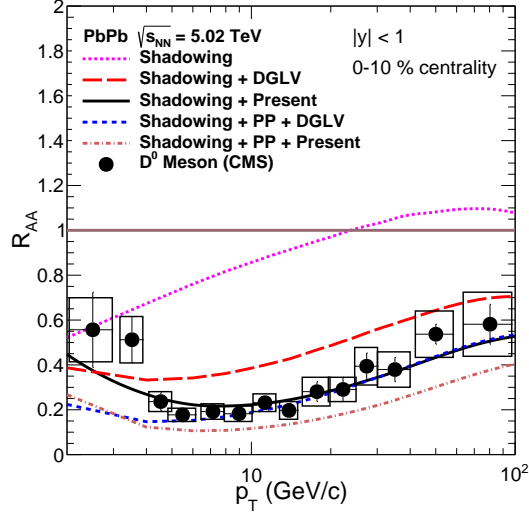


Figure 6: (color online): Nuclear modification factor R_{AA} of D^0 meson as a function of the transverse momentum p_T , obtained using energy loss (DGLV, Present, PP + DGLV and PP + Present calculation) and shadowing in PbPb collision at $\sqrt{s_{NN}} = 5.02$ TeV. The calculations are compared with the CMS data[31].

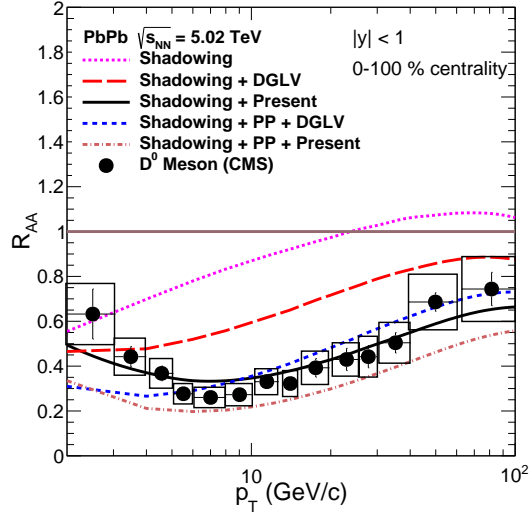


Figure 7: (color online): Nuclear modification factor R_{AA} of D^0 meson as a function of the transverse momentum p_T , obtained using energy loss (DGLV, Present, PP + DGLV and PP + Present calculation) and shadowing in PbPb collision at $\sqrt{s_{NN}} = 5.02$ TeV. The calculations are compared with the CMS data [31].

bias PbPb collision at $\sqrt{s_{NN}} = 5.02$ TeV. The calculations are compared with the CMS data [31]. The sum of the radiative energy loss by present formalism and collisional energy loss by PP formalism describes the CMS data within the uncertainties of the data. The sum of the radiative energy loss by DGLV formalism and collisional energy loss by PP formalism underestimates the B^+ meson suppression.

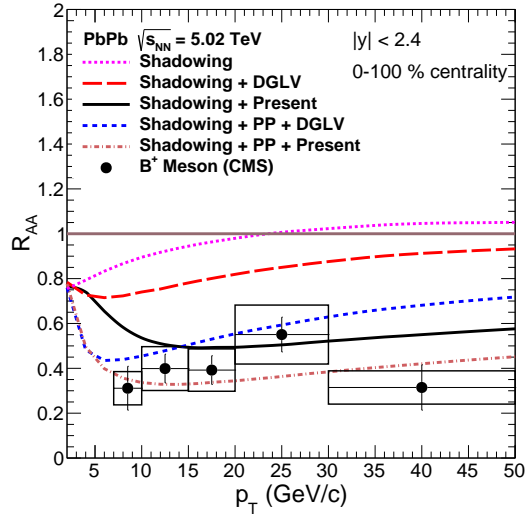


Figure 8: (color online): Nuclear modification factor R_{AA} of B^+ meson as a function of the transverse momentum p_T , obtained using energy loss (DGLV, Present, PP + DGLV and PP + Present calculation) and shadowing in PbPb collision at $\sqrt{s_{NN}} = 5.02$ TeV. The calculations are compared with the CMS data of B^+ mesons [32].

Figure 9 shows the nuclear modification factor R_{AA} of D^0 as a function of the transverse momentum p_T , obtained by including shadowing and energy loss (DGLV, Present, PP + DGLV and PP + Present calculations) in the mid rapidity region $|y| < 0.5$ for 0 - 10 % central PbPb collision at $\sqrt{s_{NN}} = 2.76$ TeV. The calculations are compared with the ALICE data [47]. Figure 10 is the same as Fig. 9 but for the case but for $|y| < 1.0$, corresponding to CMS data [48]. Figure 11 is the same as Fig. 10 but for the case in minimum bias PbPb collisions. The radiative energy loss by present formalism reproduces both the ALICE as well as CMS data without adding collisional energy loss. The radiative

energy loss by DGLV added to the collisional energy loss by PP describes the data at high p_T . The sum of the radiative energy loss by present formalism and collisional energy loss by PP formalism overestimates the measured suppression of D^0 meson.

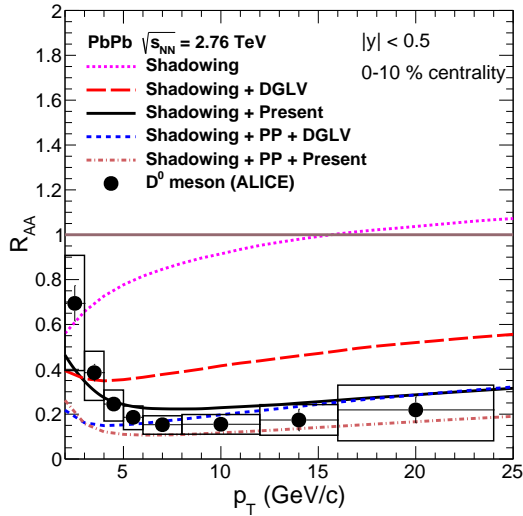


Figure 9: (color online): Nuclear modification factor R_{AA} of D^0 meson as a function of the transverse momentum p_T , obtained using energy loss (DGLV, Present, PP + DGLV and PP + Present calculation) and shadowing in PbPb collision at $\sqrt{s_{NN}} = 2.76$ TeV. The calculations are compared with the CMS data of D^0 mesons [47].

6. Conclusion

In this work, first we calculate the p_T spectra of heavy mesons in pp collision at $\sqrt{s} = 5.02$ TeV using pQCD model and make a comparison with D^0 and B^+ meson measurements of CMS. The calculations reproduce the shape of the p_T spectra of the data reasonably well. A simple hydrodynamic picture is used for QGP evolution during which the p_T spectra of heavy quarks are modified due to collision and radiative energy loss. The collisional energy loss is calculated using Peigne and Peshier formalism. The radiative energy loss is obtained using two models namely reaction operator formalism and generalized dead cone approach.

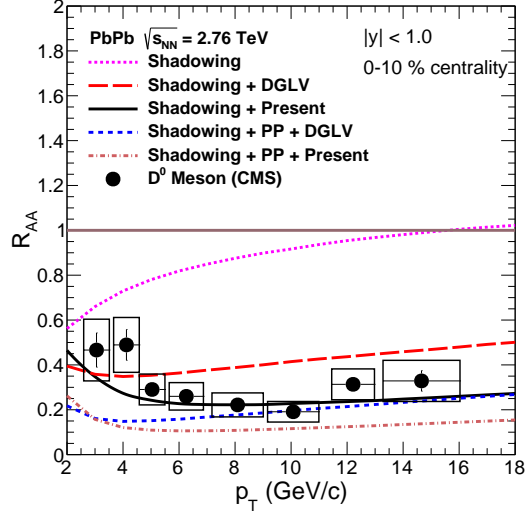


Figure 10: (color online): Nuclear modification factor R_{AA} of D^0 meson as a function of the transverse momentum p_T , obtained using energy loss (DGLV, Present, PP + DGLV and PP + Present calculation) and shadowing in PbPb collision at $\sqrt{s_{NN}} = 2.76$ TeV. The calculations are compared with the CMS data [48].

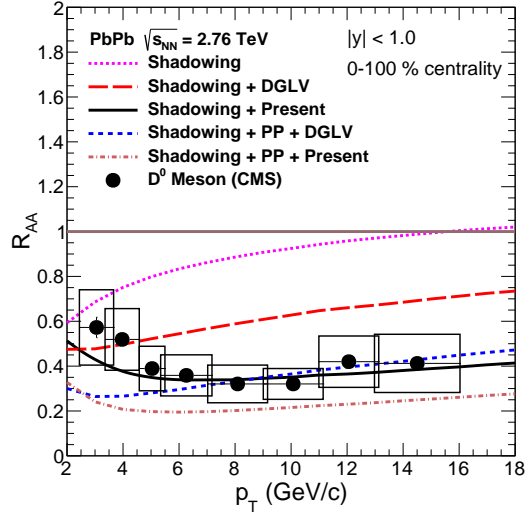


Figure 11: (color online): Nuclear modification factor R_{AA} of D^0 meson as a function of the transverse momentum p_T , obtained using energy loss (DGLV, Present, PP + DGLV and PP + Present calculation) and shadowing in PbPb collision at $\sqrt{s_{NN}} = 2.76$ TeV. The calculations are compared with the CMS data of D^0 mesons [48].

The calculations are performed for the kinematic regions covered by ALICE and CMS measurements of D meson R_{AA} in PbPb collision at $\sqrt{s_{NN}} = 2.76$ TeV and CMS measurements of D^0 and B^+ mesons R_{AA} at $\sqrt{s_{NN}} = 5.02$ TeV. The radiative energy loss from generalized dead cone approach alone is sufficient to produce D^0 meson R_{AA} at both the energies. For the case of B^+ meson, the radiative energy loss from generalized dead cone approach plus collisional energy loss gives good description of the data. It shows that collisional energy loss is significant for bottom quark. The radiative energy loss from DGLV formalism plus collisional energy loss gives good description of D^0 meson R_{AA} , but the sum of the radiative energy loss by DGLV formalism and collisional energy loss underestimates the B^+ meson suppression.

Appendix

The Born cross section is given as [2, 3]

$$\sigma_{ij} = \frac{1}{64\pi} K_{ij} \times \sum |M_{ij}|^2. \quad (13)$$

Here, K is the color averaging factor. It is $1/(N^2 - 1)^2$ for the gluon-gluon fusion process and is $1/N^2$ for the quark-antiquark annihilation process. The square of the amplitude averaged over the initial gluon polarization and color for the gluon gluon fusion is given as [2]

$$\begin{aligned} \sum |M_{gg}|^2 &= 2 g^4 (C_O B_O + C_K B_K + C_{QED} B_{QED}), \\ C_O &= N(N^2 - 1), \quad C_K = (N^2 - 1)N^{-1} \quad \text{and} \quad C_{QED} = 0, \\ B_{QED} &= \frac{t_1}{u_1} + \frac{u_1}{t_1} + \frac{4m^2 s}{t_1 u_1} \left(1 - \frac{m^2 s}{t_1 u_1}\right), \\ B_O &= \left(1 - 2\frac{t_1 u_1}{s^2}\right) B_{QED} \quad \text{and} \quad B_K = -B_{QED}. \end{aligned} \quad (14)$$

The square of the amplitude averaged over the initial quark/antiquark spins and color for the quark-antiquark annihilation process is given as [3]

$$\sum |M_{q\bar{q}}|^2 = 4 g^4 N C_F \left(\frac{t_1^2 + u_1^2}{s^2} + \frac{2m^2}{s} \right). \quad (15)$$

Here, $g(= \sqrt{4\pi\alpha})$ is the dimensionless coupling constant. $C_F(= (N^2-1)/(2N))$ is the color factor corresponding to the fundamental representation of the quarks.

References

References

- [1] Quark Matter 2014, Nucl. Phys. **A931** (2014), 1 - 1266.
- [2] W. Beenakker, H. Kuijf, W. L. van Neerven and J. Smith, Phys. Rev. D **40**, 54 (1989).
- [3] W. Beenakker, W. L. van Neerven, R. Meng, G. A. Schuler and J. Smith, Nucl. Phys. B **351**, 507 (1991).
- [4] V. Kumar, P. Shukla and R. Vogt, Phys. Rev. C **86** (2012) 054907 [arXiv:1205.3860 [hep-ph]].
- [5] J. D. Bjorken, FERMILAB-PUB-82-059-THY, FERMILAB-PUB-82-059-T.
- [6] E. Braaten and M. H. Thoma, Phys. Rev. D **44** (1991) 1298.
- [7] E. Braaten and M. H. Thoma, Phys. Rev. D **44** (1991) no.9, R2625.
- [8] A. Peshier, Phys. Rev. Lett. **97** (2006) 212301 [hep-ph/0605294].
- [9] S. Peigne and A. Peshier, Phys. Rev. D **77** (2008) 114017 [arXiv:0802.4364 [hep-ph]].
- [10] N. Armesto, C. A. Salgado and U. A. Wiedemann, Phys. Rev. D **69** (2004) 114003 [hep-ph/0312106].
- [11] N. Armesto, C. A. Salgado and U. A. Wiedemann, Phys. Rev. C **72** (2005) 064910 [hep-ph/0411341].
- [12] M. Gyulassy, P. Levai and I. Vitev, Phys. Rev. Lett. **85** (2000) 5535 [nucl-th/0005032].

- [13] M. Djordjevic and M. Gyulassy, Nucl. Phys. A **733** (2004) 265 [nucl-th/0310076].
- [14] U. Jamil and D. K. Srivastava, J. Phys. G **37** (2010) 085106 [arXiv:1005.1208 [nucl-th]].
- [15] F. Prino and R. Rapp, J. Phys. G **43** (2016) no.9, 093002 [arXiv:1603.00529 [nucl-ex]].
- [16] M. B. Gay Ducati, V. P. Goncalves and L. F. Mackedanz, hep-ph/0506241.
- [17] N. Kochelev, H. J. Lee, Y. Oh, B. Zhang and P. Zhang, Phys. Rev. C **93** (2016) no.2, 021901 [arXiv:1510.00472 [hep-ph]].
- [18] B. Abelev *et al.* [ALICE Collaboration], JHEP **1209** (2012) 112 [arXiv:1203.2160 [nucl-ex]].
- [19] B. Abelev *et al.* [ALICE Collaboration], Phys. Rev. Lett. **111** (2013) 102301 [arXiv:1305.2707 [nucl-ex]].
- [20] B. B. Abelev *et al.* [ALICE Collaboration], Phys. Rev. C **90** (2014) no.3, 034904 [arXiv:1405.2001 [nucl-ex]].
- [21] J. Uphoff, O. Fochler, Z. Xu and C. Greiner, Phys. Lett. B **717** (2012) 430 [arXiv:1205.4945 [hep-ph]].
- [22] A. Beraudo, A. De Pace, M. Monteno, M. Nardi and F. Prino, Eur. Phys. J. C **75** (2015) no.3, 121 [arXiv:1410.6082 [hep-ph]].
- [23] S. Cao, G. Y. Qin and S. A. Bass, Nucl. Phys. A **931** (2014) 569 [arXiv:1408.0503 [nucl-th]].
- [24] E. L. Bratkovskaya, T. Song, H. Berrehrach, D. Cabrera, J. M. Torres-Rincon, L. Tolos and W. Cassing, J. Phys. Conf. Ser. **668** (2016) no.1, 012008 [arXiv:1508.03887 [nucl-th]].

- [25] I. P. Lokhtin, L. V. Malinina, S. V. Petrushanko, A. M. Snigirev, I. Arsene and K. Tywoniuk, *Comput. Phys. Commun.* **180** (2009) 779 [arXiv:0809.2708 [hep-ph]].
- [26] I. P. Lokhtin, A. V. Belyaev, G. K. Eyyubova, G. Ponimatkin and E. Y. Pronina, arXiv:1601.00799 [hep-ph].
- [27] CMS Collaboration [CMS Collaboration], CMS-PAS-HIN-12-014.
- [28] K. Saraswat, P. Shukla and V. Singh, *Nucl. Phys. A* **943** (2015) 83 [arXiv:1507.06742 [nucl-th]].
- [29] J. Adam *et al.* [ALICE Collaboration], *JHEP* **1511** (2015) 205 [arXiv:1506.06604 [nucl-ex]].
- [30] J. Adam *et al.* [ALICE Collaboration], *JHEP* **1603** (2016) 082 [arXiv:1509.07287 [nucl-ex]].
- [31] CMS Collaboration [CMS Collaboration], CMS-PAS-HIN-16-001.
- [32] CMS Collaboration [CMS Collaboration], CMS-PAS-HIN-16-011.
- [33] CMS Collaboration [CMS Collaboration], CMS-PAS-HIN-16-007.
- [34] S. Wicks, W. Horowitz, M. Djordjevic and M. Gyulassy, *Nucl. Phys. A* **784** (2007) 426 [nucl-th/0512076]
- [35] R. Abir, U. Jamil, M. G. Mustafa and D. K. Srivastava, *Phys. Lett. B* **715** (2012) 183 [arXiv:1203.5221 [hep-ph]].
- [36] H. L. Lai, M. Guzzi, J. Huston, Z. Li, P. M. Nadolsky, J. Pumplin and C.-P. Yuan, *Phys. Rev. D* **82**, (2010) 074024 [arXiv:1007.2241 [hep-ph]].
- [37] I. Helenius, K. J. Eskola, H. Honkanen and C. A. Salgado, *JHEP* **1207** (2012) 073 [arXiv:1205.5359 [hep-ph]].
- [38] F. Arleo *et al.*, hep-ph/0311131.

- [39] B. Abelev *et al.* [ALICE Collaboration], JHEP **1207** (2012) 191 [arXiv:1205.4007 [hep-ex]].
- [40] K. Nakamura *et al.* [Particle Data Group Collaboration], J. Phys. G **37** (2010) 075021.
- [41] C. Peterson, D. Schlatter, I. Schmitt and P. M. Zerwas, Phys. Rev. D **27** (1983) 105.
- [42] J. F. Gunion and G. Bertsch, Phys. Rev. D **25** (1982) 746.
- [43] Y. L. Dokshitzer and D. E. Kharzeev, Phys. Lett. B **519** (2001) 199 [hep-ph/0106202].
- [44] V. Kumar, P. Shukla and R. Vogt, Phys. Rev. C **92** (2015) no.2, 024908 [arXiv:1410.3299 [hep-ph]].
- [45] J. Adam *et al.* [ALICE Collaboration], Phys. Rev. Lett. **116** (2016) no.22, 222302 [arXiv:1512.06104 [nucl-ex]].
- [46] K. Aamodt *et al.* [ALICE Collaboration], Phys. Rev. Lett. **106** (2011) 032301 [arXiv:1012.1657 [nucl-ex]].
- [47] J. Adam *et al.* [ALICE Collaboration], JHEP **1603** (2016) 081 [arXiv:1509.06888 [nucl-ex]].
- [48] CMS Collaboration [CMS Collaboration], CMS-PAS-HIN-15-005.